Characterizing the expression of cholinergic neurons within the mouse dorsal subiculum

by

Daniel Girard

A Thesis Submitted in Partial Fulfillment
of the Requirement for the Degree of

BACHELOR OF SCIENCE (HONS.)

Department of Biology, Faculty of Science
University of Victoria

We acknowledge and respect the Lək̓ʷəŋən (Songhees and Xʷsepsəm/Esquimalt) Peoples on whose territory the university stands, and the Lək̓ʷəŋən and W̱ SÁNEĆ Peoples whose historical relationships with the land continue to this day.

Characterizing the expression of cholinergic neurons

within the mouse dorsal subiculum

by

Daniel Girard

Supervisory Committee

Dr. Raad Nashmi, Supervisor
Department of Biology, University of Victoria

Dr. Terri Lacourse, Honours Advisor
Department of Biology, University of Victoria

Dr. Barbara Hawkins, Honours Advisor
Department of Biology, University of Victoria

2026

Abstract

Acetylcholine (ACh) is a neurotransmitter used for a variety of functions including muscle contraction and neurotransmission between neurons in the brain. Choline acetyltransferase (ChAT) is an enzyme that synthesizes ACh. Using a genetically modified mouse line (ChATcre::ChR2-YFP) allows us to visualize ChAT expression in brain regions due to the co-expression of yellow fluorescent protein (YFP). The dorsal subiculum expressed YFP fluorescence in adult mice, suggesting that this brain region is cholinergic despite previous research claiming otherwise. Using confocal microscopy, this study characterized YFP expression within the dorsal subiculum coupled with ChAT immunolabelling to examine whether this brain region contains cholinergic neurons. Brain sections from six ChATcre::ChR2-YFP mice between 59-95 days old of both sexes were examined. To validate correct YFP expression and ChAT labelling in other brain regions known to contain cholinergic neurons, we immunolabelled and quantified ChAT and YFP positive neurons in the primary visual cortex, the striatum, and medial habenula. We confirmed high YFP and ChAT co-expression from these brain regions. In the dorsal subiculum, we imaged YFP neurons, ChAT immunolabelled neurons, and NeuroTrace labelled neurons. Based on our results, the dorsal subiculum contained very few ChAT positive cholinergic neurons and is therefore non-cholinergic. Despite this, the sparse ChAT-labelling colocalized with YFP expression while the majority of YFP labelled cells did not co-express ChAT immunolabelling, suggesting that ChAT may have been present in the dorsal subiculum prior to adulthood. Future work should examine the subiculum during development to see if ChAT-labelling fully colocalizes with YFP expression.

Table of Contents

List of Tables

List of Figures

List of all Abbreviations

ACh – Acetylcholine

cAMP – Cyclic Adenosine Monophosphate

ChAT – Choline Acetyltransferase

ChR2 – Channelrhodopsin-2

ddH2O – Double Distilled Water

GDP – Guanine Disphosphate

GTP – Guanine Triphosphate

LTN – Laterodorsal Tegmental Nucleus

nAChR – Nicotinic Acetylcholine Receptor

NT – NeuroTrace

PBS – Phosphate-Buffered Saline

PFA – Paraformaldehyde

PPT – Pedunculopontine Tegmental Nucleus

V1B – Primary Visual Cortex

VIP – Vasoactive Intestinal Protein

YFP – Yellow Fluorescent Protein

Acknowledgments

I would like to first acknowledge the funding from the Canadian Institute of Health Research and Natural Sciences and Engineering Research Council of Canada that contributed towards purchasing materials for this study. This research would not have been possible without these groups or my supervisor, Dr. Nashmi. He has helped me gain independence working through problems while always being available to teach me skills and help solve any issues I come across. My peers in the Nashmi Lab, Foad Abazari, Adeeb Akhavan, Sema Abu Shamleh, and Lucas Copp, have also been a monumental factor in this journey. They have been a positive force helping me improve along the way. From their insight, curiosity, and kindness, they made me want to improve myself throughout my Honours Project. I would especially like to acknowledge Foad Abazari for his help in obtaining and perfusing mice, as well as for the guidance he has given me throughout this journey. Lastly, I would like to acknowledge the friends and family who have supported me throughout my undergraduate degree. Even though this year has been a period of loss, they have helped me move forward to get to this point. While I cannot mention each and every person that I have encountered throughout my research journey, I would still like to acknowledge the many hands that have shaped me into who I am today. This research has been the highlight of my undergraduate degree, and I would like to sincerely thank everyone who played a part in helping me get to this point.

1.0 Introduction

1.1 What is acetylcholine?

Acetylcholine (ACh) is an excitatory neurotransmitter that is involved in neural signalling in the brain and initiates skeletal muscular contraction at the neuromuscular junction. It is synthesized by choline acetyltransferase (ChAT), an enzyme that catalyzes the reaction between choline and acetyl CoA (Sam and Bordoni, 2023). Choline is abundant in the body from the liver or foods like egg yolks or legumes, whereas acetyl CoA can be synthesized from mitochondrial activity (Sam and Bordoni, 2023). ChAT is initially produced in the soma before being transported towards axon termini, thus allowing ACh to be synthesized and shuttled into vesicles near the presynaptic terminal via vesicular ACh transporters (Sam and Bordoni, 2023). Acetylcholinesterase degrades ACh at the synaptic cleft, thus removing excess ACh and preventing prolonged activation of ACh receptors (Sam and Bordoni, 2023).

1.2 Acetylcholine receptors

ACh mediates neuronal signalling by binding to muscarinic or nicotinic receptors (Sam and Bordoni, 2023). Nicotinic acetylcholine receptors (nAChR), named due to being activated selectively by the exogenous nicotine and the endogenous ACh, are ionotropic in nature and allow ions to flow through when activated. Neuronal nAChR consist of α and β subunits, whereas muscular nAChR have γ and δ (for fetuses) or ∈ (for adults) subunits (Sam and Bordoni, 2023). Neuronal α subunits consist of α2-α7, α9, and α10, whereas neuronal β subunits are made up of β2- β4 (Dani, 2016). α8 subunits are only found in birds. The most common nAChR subtypes are α4β2 and α7. When ACh binds to the α subunits, the receptor configuration changes to allow sodium, potassium, and calcium through the plasma membrane (Sam and Bordoni, 2023). The movement of sodium across the membrane depolarizes the cell, which can rapidly transmit information in the form of action potentials (Sam and Bordoni, 2023). The mouse dorsal subiculum, the area of interest for this study, expresses genes encoding α1, α2, α4, α7 and β2 subunits (Allen Brain Atlas, n.d.).

Muscarinic ACh receptors are activated by muscarine and ACh and signal via G protein coupled receptors (Sam and Bordoni, 2023). Attached to these receptors are heterotrimeric G proteins, consisting of $G_{\alpha/\beta/\gamma}$. Once ACh is bound, G_{α} exchanges guanine diphosphate (GDP) for guanine triphosphate (GTP), causing it to dissociate from $G_{\beta/\gamma}$ and the receptor, leading to various downstream effects (Sam and Bordoni, 2023). Muscarinic receptor subtypes M1, M3, and M5 activate phospholipase C, eventually leading to elevated intracellular calcium which is released from intracellular stores via IP3 receptors (Sam and Bordoni, 2023). Muscarinic receptors M2 and M4 inhibit adenylate cyclase, which is responsible for turning adenosine triphosphate into cyclic adenosine monophosphate (cAMP) (Sam and Bordoni, 2023). Calcium and cAMP have diverse physiological effects within the cell, including vasodilation and muscle contraction, which can thus be regulated through muscarinic receptors (Sam and Bordoni, 2023). While M1-4 are all found in the central nervous system, they can also appear on various organs (Sam and Bordoni, 2023). According to the Allen Brain Atlas, the mouse dorsal subiculum expresses genes that encode muscarinic receptor subtypes M1-4 (n.d.).

1.3 Acetylcholine functions and expression

ACh acts on many systems in the body. It is the primary messenger used in the autonomic nervous system, impacting the preganglionic sympathetic and parasympathetic nervous system, as well as the postganglionic parasympathetic nervous system (Sam and Bordoni, 2023). Additionally, ACh is responsible for activating voluntary skeletal muscle contractions and is released by motor neurons in the ventral spinal cord gray matter and cranial nuclei in the brainstem. Within the central nervous system, it can be used for tasks related to memory, motivation, arousal, and attention in various brain regions (Sam & Bordoni, 2023). When exposed to cholinergic antagonists, these processes have been shown to be affected (Broks *et al*., 1988; Klinkenberg & Blokland, 2010).

Within the mammalian brain, there are many regions that use ACh for a variety of functions. Such regions include the striatum, medial habenula, pedunculopontine tegmental nucleus (PPT), laterodorsal tegmental nucleus (LTN), and basal forebrain (Figure 1 & 2) (Woolf, 1991). Cholinergic neurons in the medial habenula project to the interpeduncular nucleus and have been shown to play a role in non-REM sleep, nicotine-withdrawal symptoms, and possibly reward and addictive behaviour (Haun *et al*., 1992; Salas *et al*., 2009; Sandyk, 1991). The striatum is known for its role in movement, and imbalances in cholinergic and dopaminergic activity can cause Parkinson's disease (Aosaki *et al*., 2010; Calabresi *et al*., 2006). Both the PPT and the LTN project to the thalamus, tectum, substantia nigra, basal forebrain, basal ganglia, raphe nuclei, locus coeruleus, sensory cranial nerve nuclei, pons, and deep cerebellar nuclei, with PPT also projecting to the reticular formation (Woolf, 1991). With its projections to the substantia nigra pars compacta (among other regions), the PPT is believed to play a role in reversal learning (Ruan *et al*., 2022). The LTN also projects onto dopaminergic neurons in the ventral tegmental area which modulates reward-related behaviours (Coimbra *et al*., 2021). The basal forebrain contains cholinergic projection neurons, which innervate neurons in the prefrontal cortices, hippocampi, subicular complex, and amygdala, among other areas. The basal forebrain regulates attention and memory (Eickhoff *et al*., 2022; Woolf 1991). Alterations in ACh and cholinergic innervation have been found to be prominent in various psychotic disorders and neurological conditions, such as schizophrenia and Alzheimer's disease (Eickhoff *et al*., 2022; Huang *et al*., 2022). Because ACh is prominent throughout the body, studying regions that use ACh is important to understand their role in health and diseases and to better devise strategies to mitigate their symptoms.

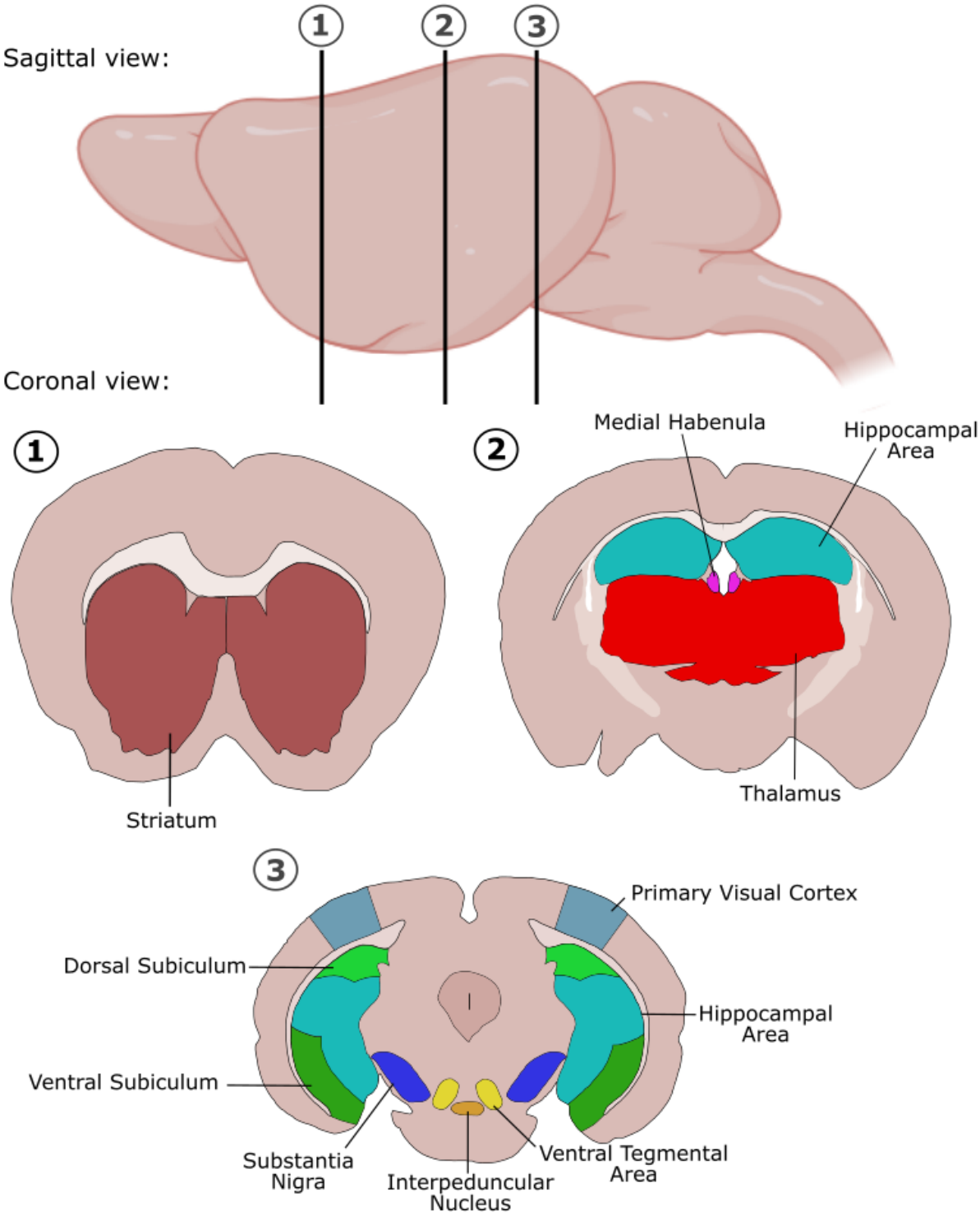

Figure 1. Coronal view of various brain regions and their corresponding sagittal location. Coronal brain sections adapted from the Allen Brain Atlas (n.d.). Certain assets created using BioRender.com.

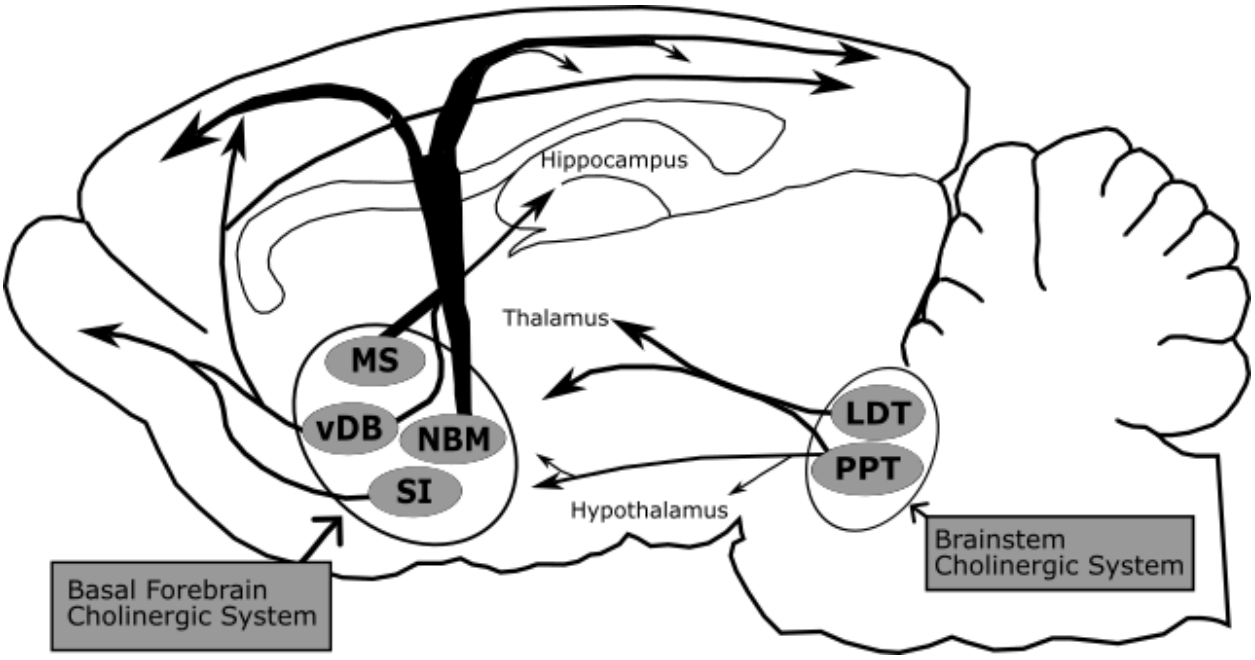

Figure 2. Cholinergic projection systems in the mouse brain. Figure adapted from Villano *et al*. (2017).

Using a transgenic mouse line, particularly ChATcre::ChR2-YFP, it is possible to visualize cholinergic neurons throughout the brain (Figure 3). Whenever ChAT is expressed, cre-recombinase is synthesized which allows channelrhodopsin-2 (ChR2) and yellow fluorescent protein (YFP) to be expressed via the Cre-lox system. When excited by blue light, YFP emits wavelengths between 521-550 nm peaking at 528 nm (Thermofisher Scientific, n.d.; Lumencor, 2021). By using this transgenic mouse line, it is possible to visualize ChAT expression within neurons and neuropil.

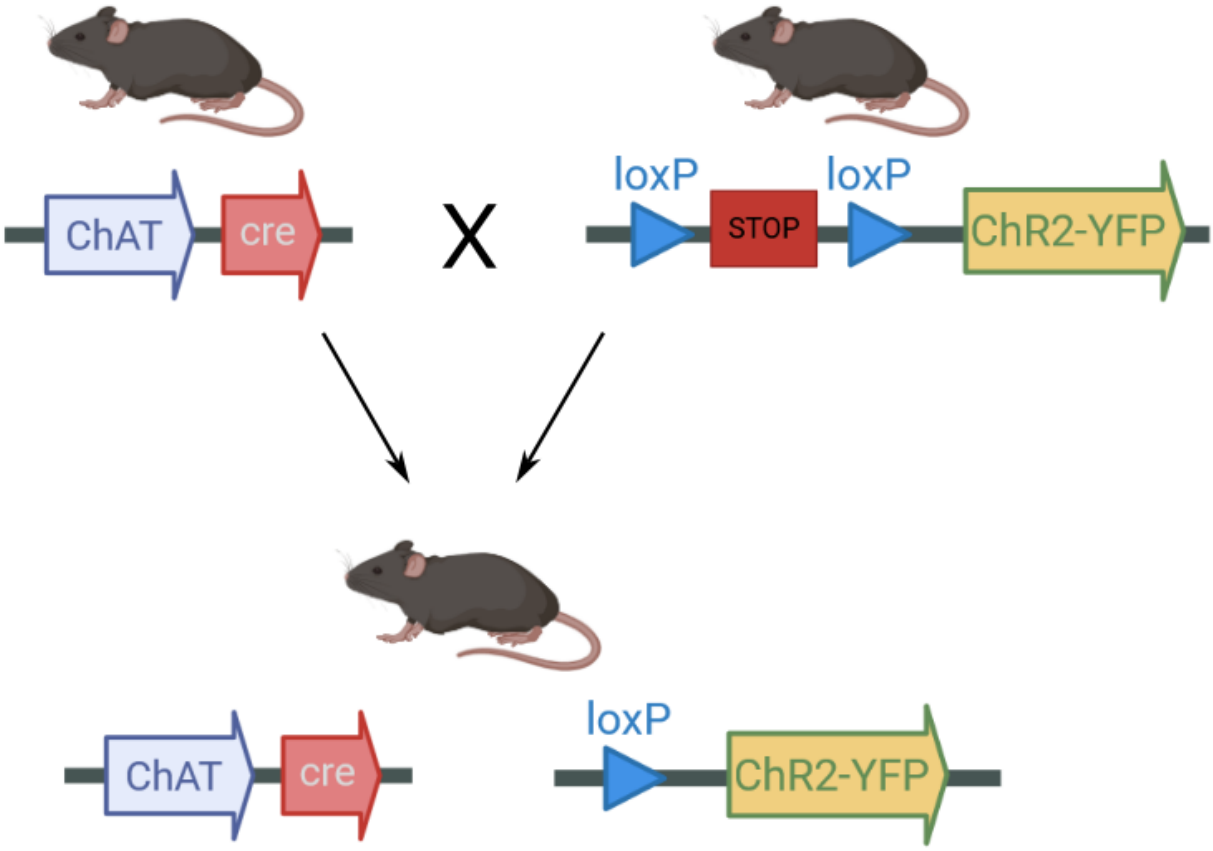

Figure 3. Creation of ChATcre::ChR2-YFP transgenic mouse line by breeding ChATcre and ChR2-YFP transgenic mice. Certain assets created using BioRender.com.

A study by a previous Honour student in the Nashmi Lab found that YFP is expressed in the dorsal subiculum, which would suggest that the subiculum is cholinergic (unpublished data). However, it was not clear whether YFP was expressed in neuronal cell bodies or in long range projection afferents from remote brain regions.

1.4 What is the subiculum?

In the mouse, the subiculum is located approximately within -2.8 to -4.5 mm relative to bregma and resides near the hippocampus (Franklin & Paxinos, 2008). It is part of the subicular complex alongside the presubiculum, parasubiculum, and

postsubiculum[1] (Aggleton & Christiansen, 2015). Anteriorly, the subiculum is divided into dorsal and ventral components, each containing a pyramidal layer, molecular layer, and stratum radiatum (Allen Brain Atlas, n.d.). Due to its proximity and shared connectivity, the subiculum was believed to support the hippocampus in its general functions (Aggleton & Christiansen, 2015). Despite receiving the majority of its inputs from dense CA1 hippocampal pyramidal neurons, the subiculum projects to many of the same areas as the hippocampus, including the retrosplenial cortex, midline thalamic nuclei, hypothalamus, and postrhinal cortex, to name a few, and even to areas where the hippocampus does not reach, like the anterior thalamic nuclei and mamillary bodies (Aggleton & Christiansen, 2015). It can even regulate hippocampal activity through its projections to the entorhinal cortex and CA1 field (Commins *et al*., 2002). The subiculum is believed to contribute towards memory and learning through its projection to the medial diencephalon and anterior thalamic nuclei (Aggleton & Christiansen, 2015; Barnett *et al*., 2021).

1.5 Cholinergic neurons in the subiculum

Although the subiculum is innervated by medial septal and vertical diagonal band ChAT fibers of the basal forebrain, it is not believed to be cholinergic itself (Woolf, 1991). Despite this, strong YFP fluorescence was shown to be expressed in the dorsal subiculum in ChATcre::ChR2-YFP mice from a previous study in the Nashmi lab (unpublished data), which suggests that cholinergic neurons may also be expressed. There are a few possibilities available to explain the inconsistency between the scientific literature and the results found in our lab.

One possibility is that the subiculum is cholinergic and has been overlooked in its inherent characteristics by the scientific community. Another option is that the subiculum is not a cholinergic nucleus but receives heavy cholinergic innervation originating from other brain regions. A third possibility is that the subiculum is non-cholinergic and that

[1] The postsubiculum is part of the rodent subicular complex and is sometimes considered as the presubiculum. Primates only have the presubiculum, parasubiculum, and subiculum (Aggleton & Christiansen, 2015).

our ChATcre::ChR2-YFP transgenic mouse line is ectopically expressing YFP in regions that do not express ChAT. To determine whether cholinergic neurons are present in the subiculum and to what degree, this study will examine ChAT-expression using immunohistochemistry on the dorsal subiculum. Additionally, we will be examining the striatum, medial habenula, and primary visual cortex (V1B) as they have been previously shown to be cholinergic (Woolf, 1991).

Previous studies in our lab using goat antibodies directed to ChAT have shown ChAT labelling in the medial habenula, V1B, and striatum, but it has yet to be seen if it will be similar in the subiculum. To this end, we will compare goat and rabbit antibodies to see which is the most reliable for visualizing ChAT neurons. Following this, we will image and calculate the density of cholinergic neurons in the dorsal subiculum and compare it with the subiculum's overall neuronal density using NeuroTrace (NT) to visualize all cell bodies present. Furthermore, we will also find the cholinergic density of the V1B, and the amount of colocalization between ChAT and YFP cell bodies in the striatum to determine if ChAT cell body quantification is consistent with YFP expression in this region. Based on ChAT-labelling, the dorsal subiculum will be considered cholinergic if it contains a cluster of numerous ChAT labelled neuronal cell bodies which should be co-expressed with the YFP-containing neurons.

1.6 Objectives and hypotheses

The objective of this study is to determine whether the mouse dorsal subiculum expresses cholinergic cell bodies. To this end, I compared the expression of cell bodies labelled by YFP and ChAT in regions known to be cholinergic. This includes the striatum, medial habenula, and V1B, in addition to the dorsal subiculum. My hypothesis is that brain regions marked by ChAT antibodies will colocalize with areas expressing YFP. Additionally, I compared the number of ChAT neurons in V1B with the number of YFP neurons expressed, as well as seeing what fraction of cell bodies colocalize in the striatum. I also imaged the dorsal subiculum directly to see the difference between ChAT and YFP expression. To get a better sense of how many neurons in the dorsal subiculum are cholinergic, I found the overall number of neurons present and compared

it with the number of cell bodies immunolabelled with ChAT. Assuming the dorsal subiculum is cholinergic, we should see a similar number of cell body clusters in YFP and ChAT labelled neurons.

2.0 Materials and Methods

2.1 Brain collection

All experiments were performed according to an animal protocol (AE-24-020) approved by the animal care committee at the University of Victoria and in accordance with the Canadian Council of Animal Care Guidelines. We used ChATcre::ChR2-YFP knock-in mice, which is a cross between the ChATcre mouse line (JAX# 031661) and the ChR2-YFP mouse line (JAX# 024109), and bred to homozygosity for both genes. We collected brains from six adult ChATcre::ChR2-YFP mice between 59 and 95 days old. Two of the ChATcre::ChR2-YFP mice were female, whereas the rest were male. While under deep isoflurane anesthesia (Fresenius Kabi), ChATcre::ChR2-YFP transgenic mice were perfused intracardially with phosphate-buffered saline (PBS) (8 g NaCl, 1.44 g Na_2HPO_4, 0.2 g KCl, 0.24 g KH_2PO_4, diluted in ddH_2O, pH 7.6) and 4% paraformaldehyde (PFA) diluted in PBS (Electron Microscopy Science) prior to brain removal to preserve the brain for slicing and imaging. Once perfused, the brain was removed, refrigerated at 4°C, and immersed in 4% PFA overnight while wrapped in aluminum foil to prevent photobleaching fluorescent proteins. Brains were immersed in PBS the following day until further use.

Table 1. Mouse ID, age, sex, and position relative to bregma used to quantify cholinergic neurons in the dorsal subiculum.

Mouse ID	**Age (days)**	**Sex**	**Bregma[2] (mm)**
ChATcre::ChR2-YFP-1	70	M	-3.8 & -3.28
ChATcre::ChR2-YFP-2	95	M	-3.52
ChATcre::ChR2-YFP-3	95	M	-2.92
ChATcre::ChR2-YFP-4	95	M	-3.28
ChATcre::ChR2-YFP-5	62	F	-3.52
ChATcre::ChR2-YFP-6	59	F	-3.52 & -3.64

[2] These bregma positions are only considering those that were used to quantify ChAT neurons in the dorsal subiculum.

2.2 Slicing

Prior to slicing, part of the cerebellum and frontal lobe were removed to provide a stable surface for the brain to sit upright and to reduce the distance to the targeted brain regions. Brains were immersed in 3% agar solution (diluted in ddH_2O) and glued onto the stage of a Vibratome Series 1000 Sectioning System (Technical Products International). The vibratome was set to an amplitude of 0.4 mm and a speed of 2 mm/s. Brains were sliced coronally at a thickness of 200 µm. Slices of the striatum, medial habenula, and dorsal subiculum were collected between +1.1 to +0.38 mm, -1.2 to -1.8 mm, and -2.8 to -3.8 mm relative to bregma, respectively. Slices were immersed in glycerol antifreeze solution (0.69 g Na_2HPO_4, 0.39 g NaH_2PO_4, 100 mL ddH_2O, 75 mL ethylene glycol, 75 mL glycerol, pH 7.5) and stored at -18 °C until further use.

2.3 Immunohistochemistry

Brain slices were rinsed three times with PBS whilst on a Labline 3520 Orbital Shaker (Hyland Scientific) for 10 min each. Once PBS was removed, 250 µL of 0.25% Triton X-100 solution (diluted in PBS) was added to each slice for 10 min. Slices were again rinsed with PBS three times for 10 min to remove the Triton X-100 solution. 250 µL of 10% donkey serum (Jackson ImmunoResearch, cat #017-000-121) diluted in PBS was applied for 30 min followed by 250 µL of 1:250 primary antibody solution in 3% donkey serum (diluted in PBS) and left on the shaker overnight. Slices were then rinsed three times with PBS for 10 min each to remove primary antibody solution and applied with 250 µL of 1:500 secondary antibody solution in 3% donkey serum (diluted in PBS). After being left overnight, slices were rinsed with PBS three times for 10 min before being mounted onto a labelled Superfrost Plus microscope slide. PBS was evaporated at 37 °C using a Fisher Isotemp Mechanical Convection oven model 350D (Thermo Fisher Scientific), then slices were immersed in Immu-Mount (pH 8.0-8.5) (Epredia) and a cover slip was applied. Parafilm was used to hold the cover slip in place while the Immu-Mount dried, and was later sealed with nail polish to preserve slices.

Goat-anti-ChAT (Millipore, cat #AB144P) and donkey-CY5-anti-goat were used to label ChAT neurons and were compared to rabbit-anti-ChAT (abcam, cat #ab178850) and donkey-CY5-anti-rabbit. Subicular cell bodies were labeled with NeuroTrace 435/455 Blue Fluorescent Nissl Stain (Thermo Fisher Scientific, cat #N21479) using a similar method as described above, but with the use of a Nissl stain.

2.4 Confocal imaging

Following immunohistochemistry, cover-slipped brain sections were examined using a Nikon C1-si confocal system attached to a Nikon Eclipse Ti-E inverted microscope using EZ-C1 acquisition software. Images were taken using a Nikon Plan Fluor 10X (0.3 NA), a Nikon Plan Apo 20X (0.75 NA), and a Nikon Plan Apo 60X (1.4 NA) objectives. Acquired images were averaged over 5 sweeps for a single optically sectioned image and an average of 3 sweeps per optical section in a z-stack of images. The pinhole was set at either small (30 µm diameter) or medium (60 µm diameter); the spectral gain was set to 220; the digital resolution of the image was taken at 1024 x 1024 pixels; and a 1 µm step size was set when imaging a z-stack. NT was excited with a diode laser emitting at 405 nm wavelength and fluorescence was collected between 451 nm and 551 nm. The CY5-anti-goat secondary antibody was excited using a 640 nm diode laser and emission fluorescence was collected between 650 nm and 750 nm. YFP was excited with the 488 nm wavelength line of an argon laser and the fluorescence emission was collected between 511 nm and 611 nm. The brain regions imaged included the dorsal subiculum, V1B, medial habenula, and striatum. NT-labelled images were spectrally unmixed using a spectral unmixing algorithm in the Nikon EZ-C1 software and reference spectra of EYFP and NT. In confocal images from brain sections with YFP and CY5-fluorescent labels, each fluorescent label was spectrally segmented.

2.5 Data analysis

Images were analyzed using ImageJ (Schneider *et al*., 2012). A Gaussian Blur was applied (sigma radius = 2.00 µm) to smooth edges and make identifying neurons easier in the next steps. The Subtract Background function (Rolling Ball radius = 25.0 pixels) was used to remove background noise and create a consistent background to

apply a threshold to further separate labelled structures from background noise based on pixel intensity. An Isodata threshold algorithm was applied to NT-labelled neurons. ImageJ's Watershed function was applied to better estimate actual neuronal size from the provided threshold. From there, Analyze Particles was applied to automatically count the number and size of neurons obtained from the threshold in a selected area. Shapes created by the threshold were only considered if they were greater than 80 μm^2 in area for NT-labelled slices. The estimated number of neurons within a z-stack was calculated by dividing the total volume of thresholded NT labelling in the entire stack divided by the average volume of a single neuron(on the assumption that the neuron is a perfect sphere), The average volume of a neuron was estimated by determining from each z stack the average cross sectional area of NT labelled cells. Then assuming a spherical shape for a cell, the radius was calculated and from this the average volume of an NT labelled cell was calculated. Neuronal density was found by dividing the calculated number of neurons in a stack by the volume of the selected area. In cases where neuronal density was minimal, such as ChAT immunolabelled neurons in the dorsal subiculum, the cell bodies were instead counted manually. Data was graphed in RStudio (Posit Team, 2026). All figures were made using Inkscape (Inkscape Project, 2026).

3.0 Results

3.1 YFP expression in the subiculum

As shown in Figure 4, the dorsal subiculum was found to prominently express YFP along with the supramammillary nucleus, commonly known to contain ChAT cells, and the fasciculus retroflexus, a bundle of cholinergic fibres that project from the medial habenula to the interpeduncular nucleus (Woolf, 1991). Examining YFP expression with a greater objective lens shows cell bodies alongside subcellular structures, including axons and dendrites (Figures 5, 6, & 7). Axons appear to be thin in appearance and contain *en passant* synaptic boutons, as shown by the sparse dots along their axons that resembles beads on a string (Figure 6). Dendrites are thicker and have dendritic spines, which appear as tiny dots along their length (Figure 7). These structures appear uniformly throughout the dorsal subiculum.

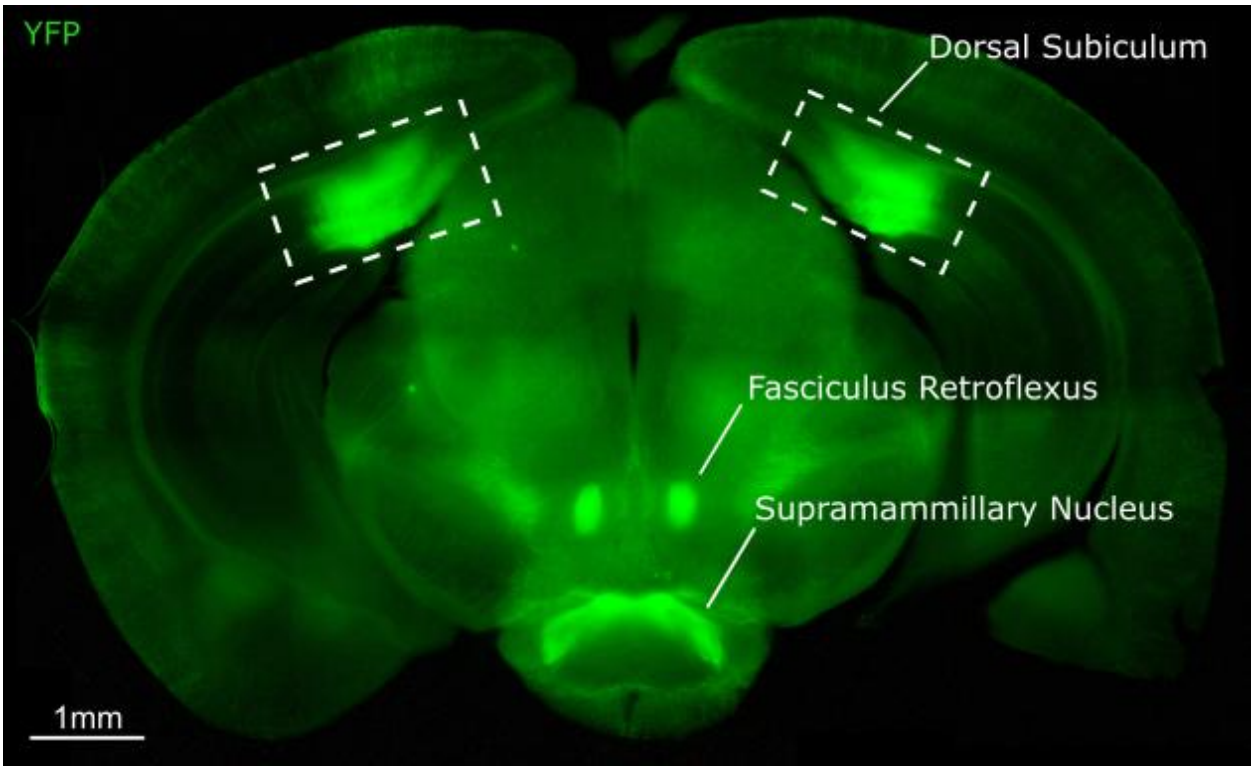

Figure 4. Coronal view of the ChATcre::ChR2-YFP mouse midbrain. Area within the white dotted box is the dorsal subiculum. Montage created with a 10X objective lens.

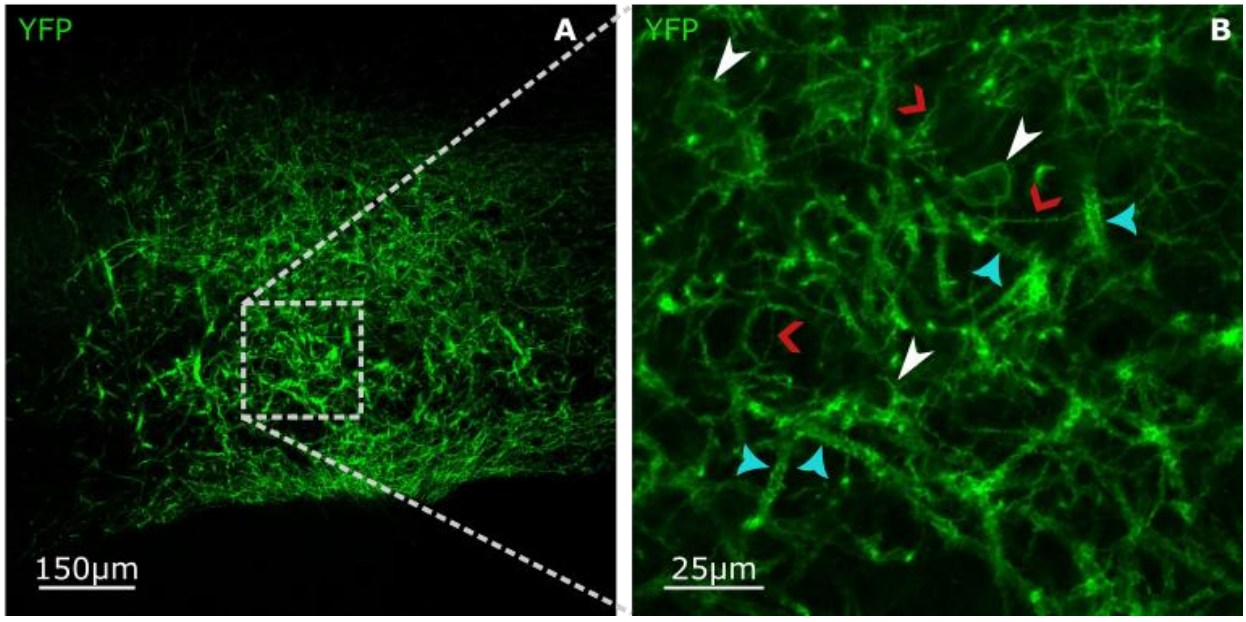

Figure 5. YFP expression in the dorsal subiculum with a 20X objective lens with a field of view of 636.5 µm x 636.5 µm (**A**) and 152.76 µm x 152.76 µm (**B**). White arrows show cell bodies, blue arrows represent dendrites, and red arrows point towards axons.

3.2 Morphology of subicular neurons

Examining YFP subicular expression in greater detail, various neuropil can be seen using a 20X or 60X objective. In particular, dendrites and axons are found in great detail (Figures 5, 6, & 7). Axons can be identified from their thin widths (~1 nm wide) (Muzio *et al*., 2022), whereas dendrites are characterized by their thick widths (~2.7 µm wide) which taper off (~ 0.5 µm wide) (Barlett & Banker, 1984). Along the fine axons, various swellings resembling *en passant* synaptic boutons can be seen (Figure 6). Dendritic spines are present along dendrites and act as the post-synaptic surface to receive innervation (Figure 7).

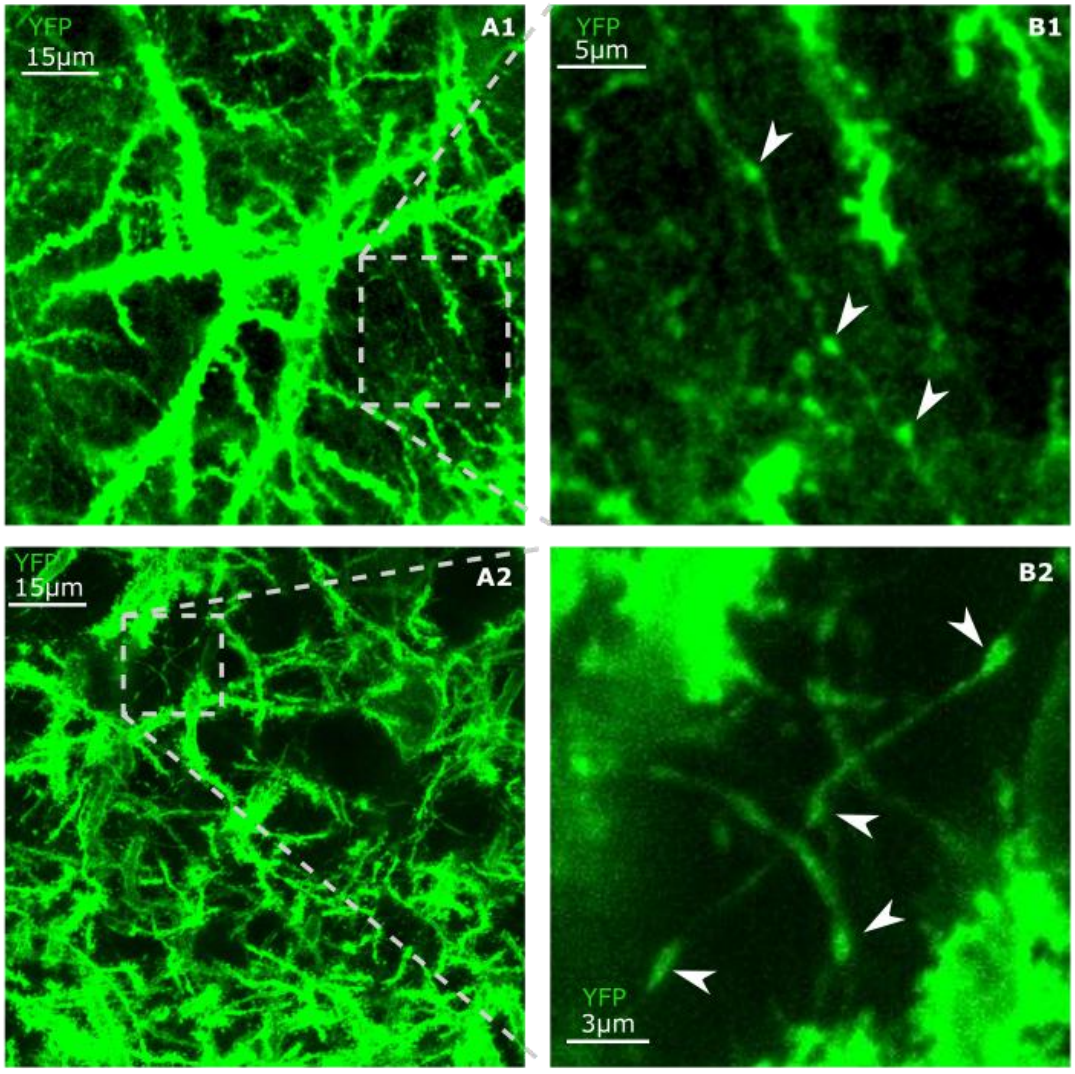

Figure 6. En passant presynaptic boutons visualized with YFP in the dorsal subiculum. Image taken with a 20X objective lens with a field of zoom of 150.6 µm x 150.6 µm (**A1**), and a 60X objective lens at a field of zoom of 99.9 µm x 99.9 µm (**A2**). Original images were enlarged to better display axons (**B**). White arrows show synaptic boutons. Image contrast increased to better visualize axon and synaptic boutons. Figure created using a z-stack maximum intensity projection with a depth of 5 µm (**1**) and 6 µm (**2**).

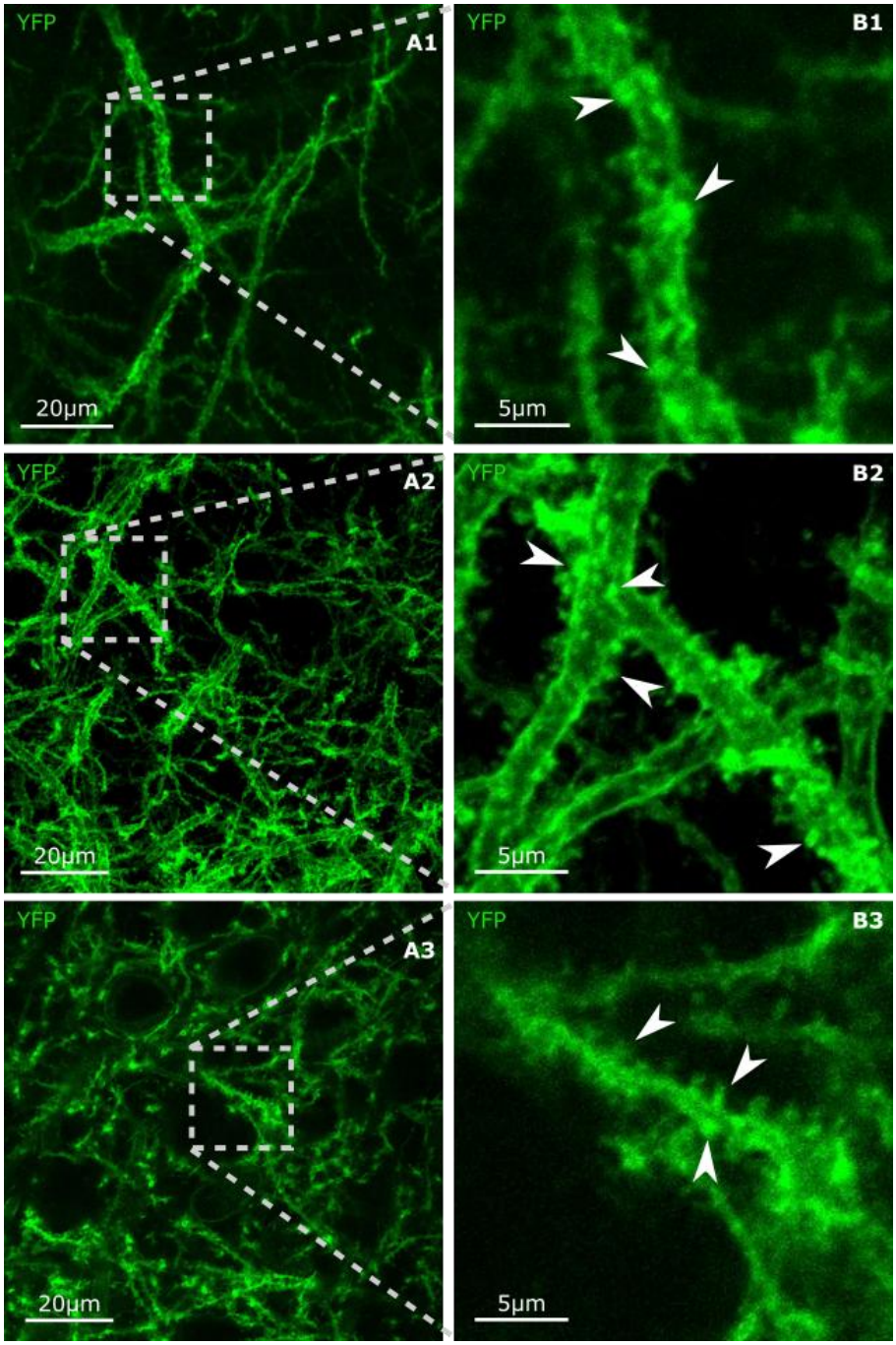

Figure 7. Dendrites and dendritic spines visualized with YFP in the dorsal subiculum. Images were taken with a 20X objective lens with a field of zoom of 150.6 μm x 150.6 μm (**1**), and a 60X objective lens at 99.9 μm x 99.9 μm (**2** & **3**). Original images were enlarged to better display dendrites (**B**). White arrows show dendritic spines. Figure created using a z-stack maximum intensity projection with a depth of 5 μm (**1**), 16 μm (**2**), and 1 μm (**3**).

3.3 Testing goat vs rabbit antibodies

To ensure that ChAT-labelling was accurate, goat and rabbit primary antibodies were compared in the dorsal subiculum. Both rabbit-anti-ChAT and goat-anti-ChAT labelled similar numbers of cell bodies within the dorsal subiculum (Figure 8), with goat-anti-ChAT managing to label more substructures. Due to its slightly superior labelling of neuropil, goat-anti-ChAT was used for future quantification of cell bodies. Thus, cholinergic neurons would be quantified using goat-anti-ChAT in the dorsal subiculum and the V1B. Despite the slight differences in labelling, both could realistically be used to examine subicular cell bodies. While examining known cholinergic-positive regions in the brain, ChAT-labelling seems to match YFP expression (Figure 9). While the medial habenula is densely packed with cholinergic neurons which makes identifying individual cell bodies difficult, the overall shape of the ChAT-labelled brain region seems to match those visualized with YFP. The striatum, in comparison, has many clearly visible cell bodies which can be differentiated. Most ChAT-labelled YFP neurons in the striatum are found to colocalize with a cell body visualized by YFP. Since the V1B has few cholinergic neurons, it is much easier and quicker to identify cell bodies. Both YFP and ChAT seem to colocalize in V1B.

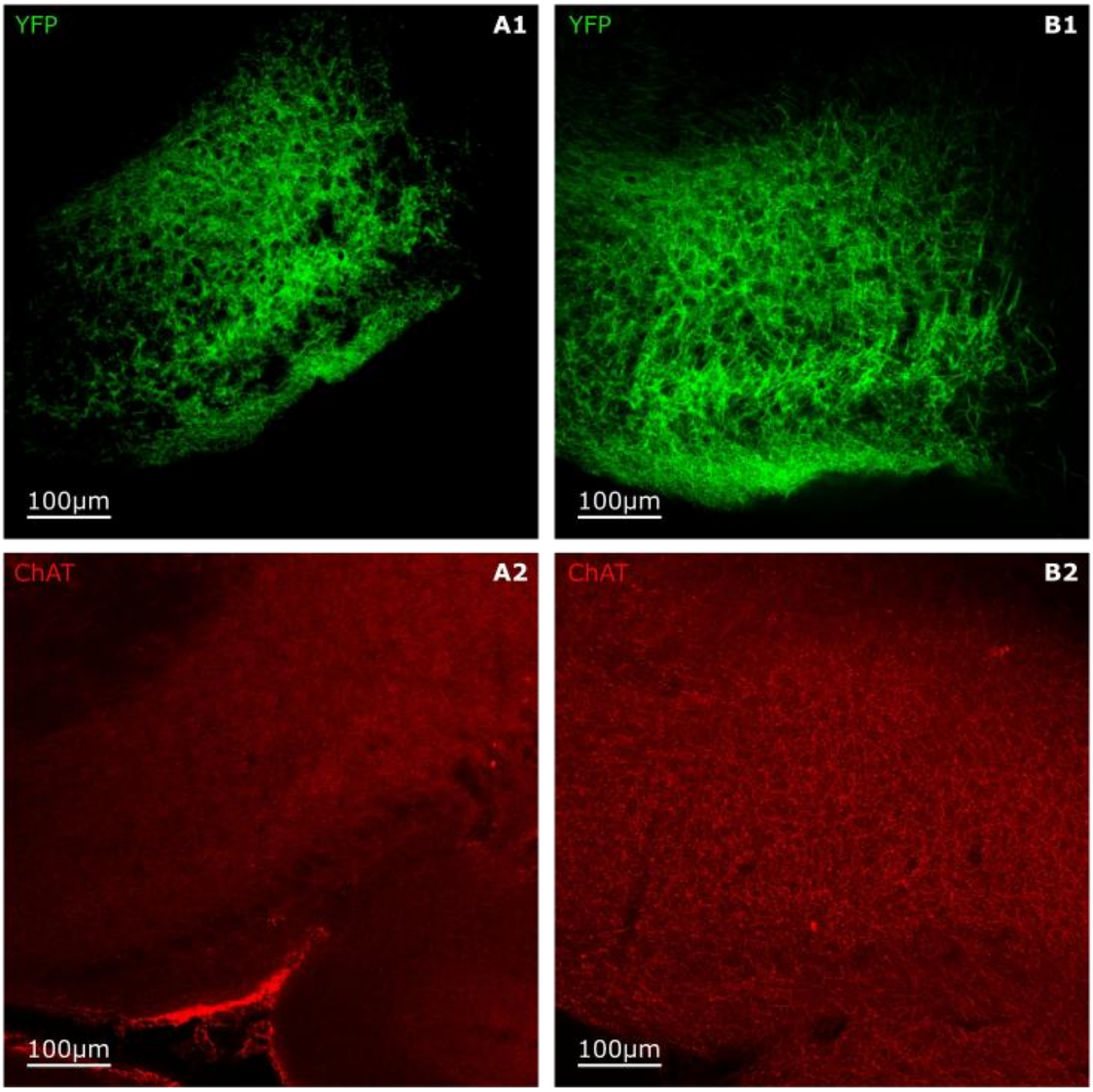

Figure 8. Rabbit-anti-ChAT (**A2**) and goat-anti-ChAT (**B2**) immunolabelling in the dorsal subiculum compared with YFP expression (**1**). Images were taken with a 20X objective lens with a field of view of 636.5 µm x 636.5 µm.

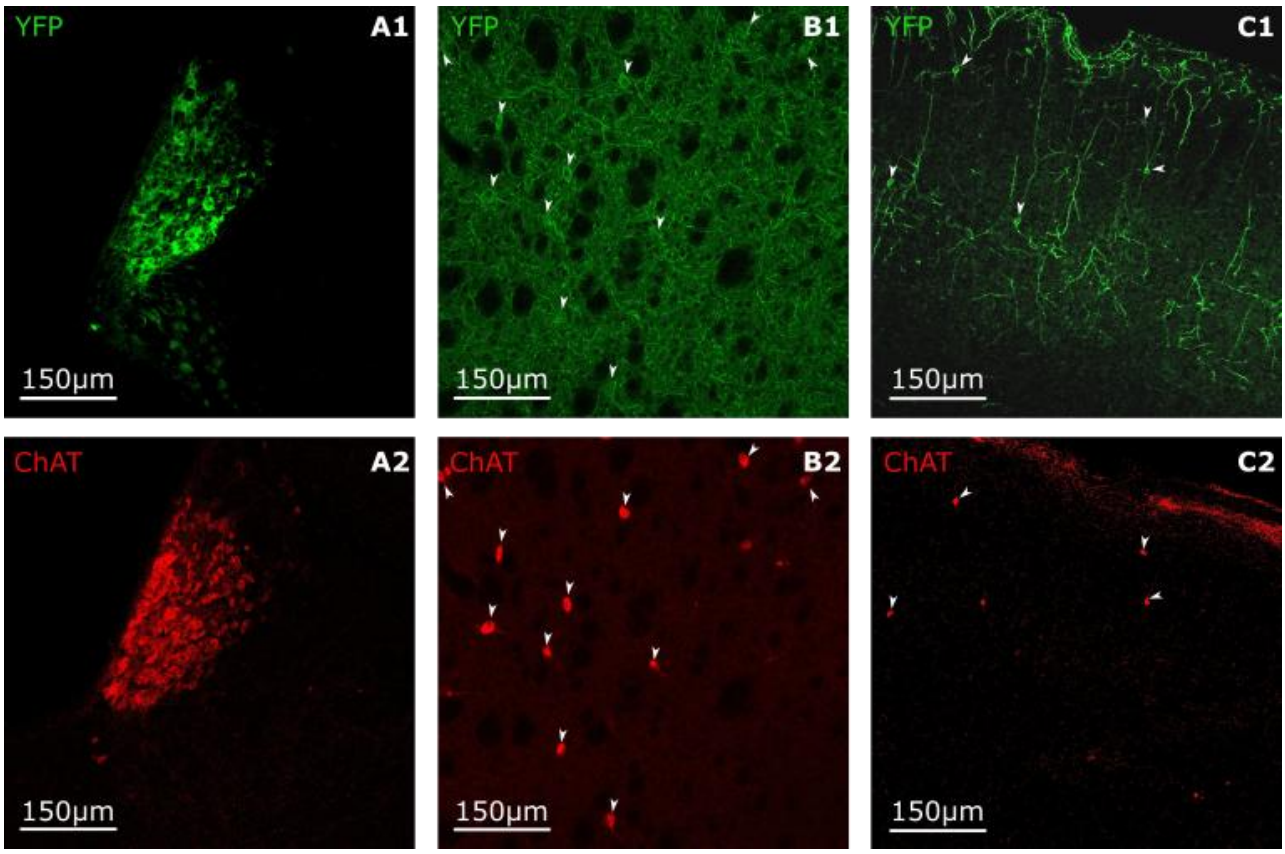

Figure 9. YFP expression (**1**) and ChAT labelling (**2**) in the medial habenula (**A**), striatum (**B**), and V1B (**C**). White arrows show overlapping cell bodies. Images taken with a 20X objective lens with a field of view of 636.5 µm x 636.5 µm.

3.4 Cell quantification

NT labelling in the dorsal subiculum produced adequate staining of subicular neurons (Figure 10). Quantification of the dorsal subiculum and V1B can be found in Table 2. The average number of NT-labelled cell bodies was found to be 375 (±16) within the dorsal subiculum (n = 11 hemispheres from six mice). The average density was found to be 99,940 (±1,478) neurons per mm^3. Using the area of the pyramidal layer of the dorsal subiculum (where most cell bodies seemed to be located) from the Allen Brain Atlas (n.d.) and Simpson's Rule, the dorsal subiculum was found to have an approximate volume of 0.49 mm^3. With this volume and the density of NT-labelled neurons, the dorsal subiculum should contain 48,487 neurons, overall.

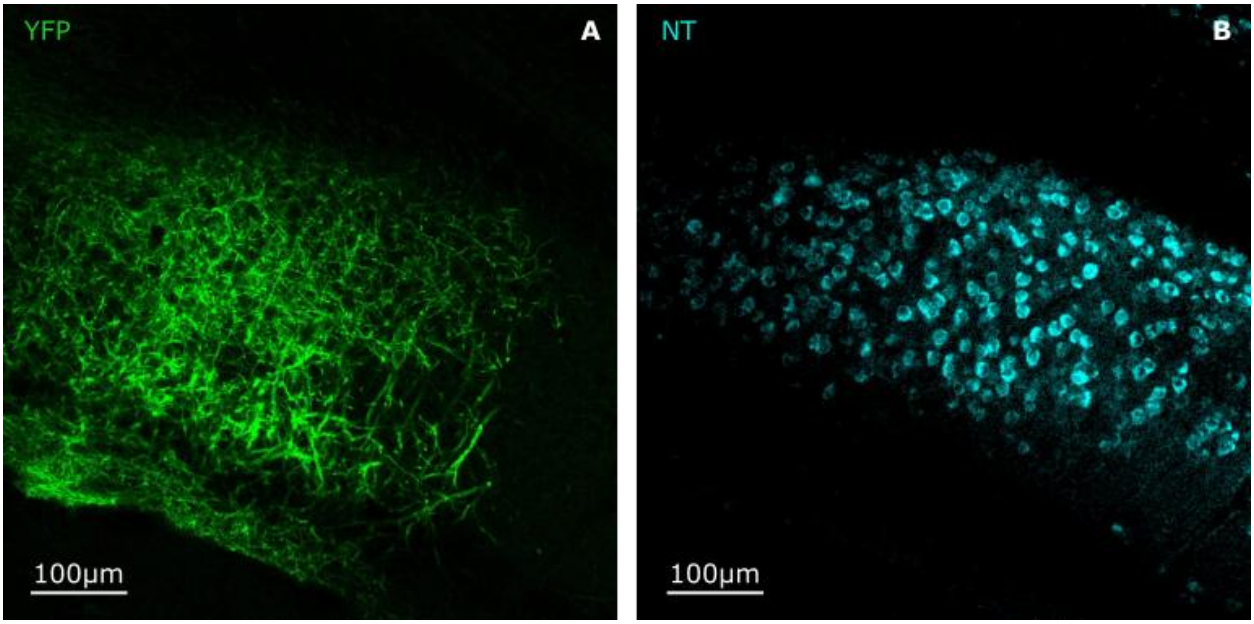

Figure 10. YFP (**A**) and NT co-expression (**B**) in the dorsal subiculum. Single frame images were taken with a 20X objective lens with a field of view of 636.5 µm x 636.5 µm.

Table 2. Quantification of NT and ChAT in the dorsal subiculum, and YFP and ChAT in V1B. NT results were automatically quantified using ImageJ, whereas YFP and ChAT labelling in V1B and dorsal subiculum were manually counted. Each field of view was 636.5 µm x 636.5 µm.

	NT-labelling (dorsal Subiculum)	ChAT-labelling (dorsal Subiculum)	ChAT-labelling (V1B)	YFP-labelling (V1B)
Average Neuron Count	374.6	4.8	32.1	39.0
Standard Error	16.0	0.2	1.3	1.1
Average Density (Neurons/mm^3)	99,940.7	885.2	4,535.3	5,536.4
Standard Error	1,477.7	43.3	186.3	174.5
Range of Depths of z-stacks Imaged (µm)	10 to 34.5	25 to 32*	28 to 32	28 to 32
Number of Hemispheres	11	12	8	8
Number of Mice	6	6	4	4

*One hemisphere only measured 14 µm of a z-stack.

In comparison, the average number of cholinergic neurons within the dorsal subiculum (Figure 11) was found to be 5 (±0.23) neurons with a density of 885 (±43) neurons per mm^3 (n = 12 hemispheres from 6 mice). Using the volume calculated above, the dorsal subiculum should contain 429 cholinergic neurons, making up approximately 0.89% of all neurons within the dorsal subiculum. Despite the overwhelming number of neurons expressing YFP, too few ChAT-labelled neurons are present to consider the dorsal subiculum cholinergic. Interestingly, the ChAT-labelled neurons that are present tend to colocalize with YFP cell bodies, suggesting that YFP is not randomly expressed.

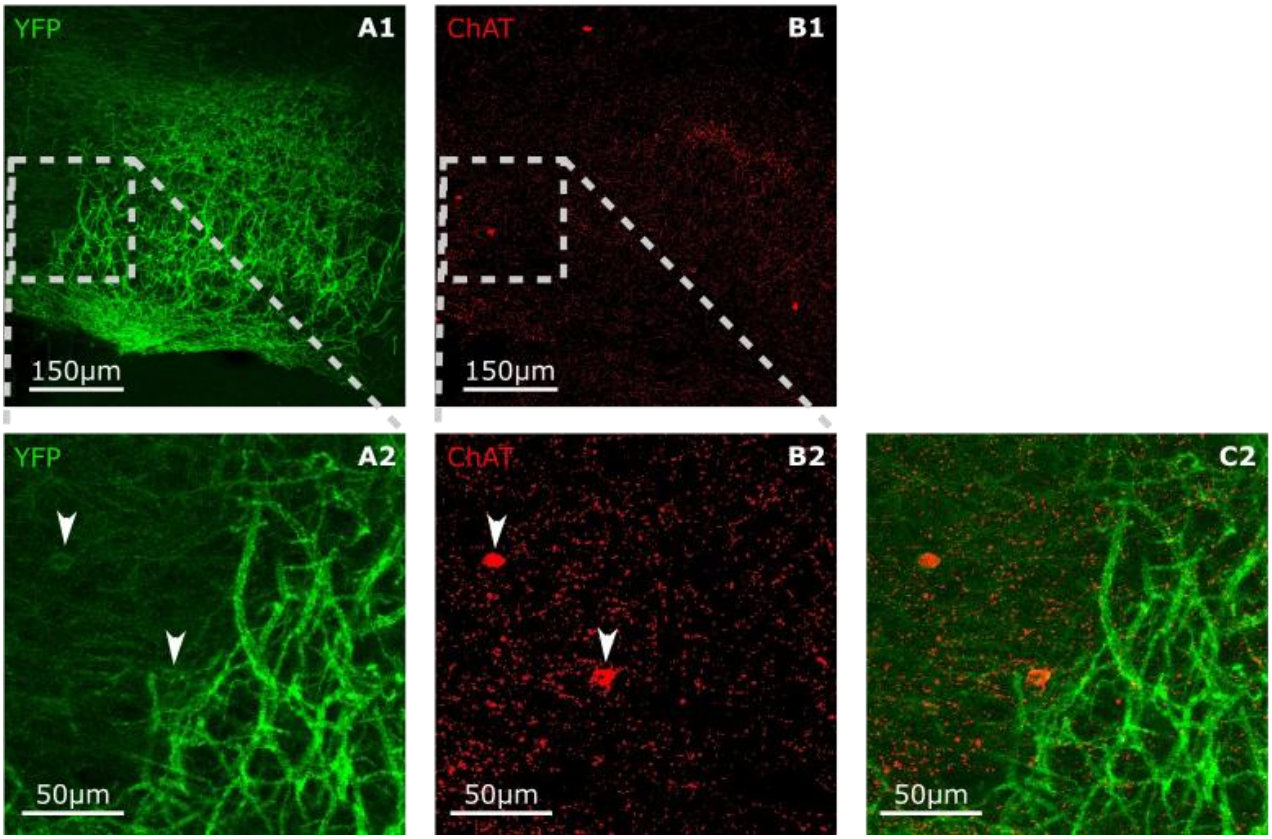

Figure 11. YFP and ChAT co-expression in the dorsal subiculum (**A**, **B**, **C**). Images were taken with a 20X objective lens with a field of view of 636.5 μm x 636.5 μm (**1**). Original images were enlarged to better display cell body colocalization (**2**). Figure created using a z-stack maximum intensity projection with a depth of 6 μm.

Examining V1B (Figure 12), ChAT-density was calculated to be 4,535 (±186) neurons per mm^3, with 32 (±1) neurons counted on average (n = 8 hemispheres from 4 mice). In comparison, 39 (±1) YFP neurons were expressed, leading to a density of 5,536 (±174) neurons per mm^3 (n = 8 hemispheres from 4 mice). The ratio of ChAT-to-YFP cell bodies is 0.83 (±0.03).

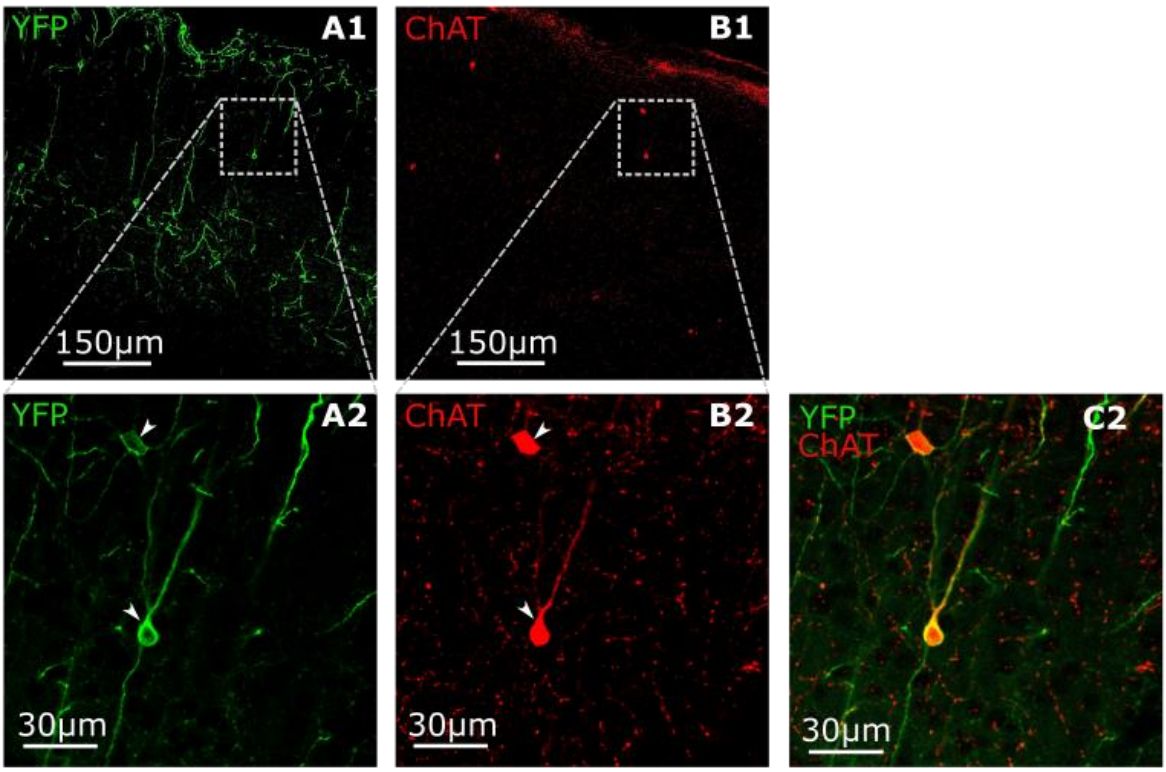

Figure 12. YFP (**A**, **C**) and ChAT (**B**, **C**) co-expression in the V1B. Single frame images were taken with a 20X objective lens with a field of view of 636.5 μm x 636.5 μm (**1**) and 152.8 μm x 152.8 μm (**2**).

When assessing the striatum in greater detail (Figure 13), 81.2% of ChAT cell bodies were shown to colocalize with YFP neurons compared to 89.3% of YFP cell bodies overlapping with ChAT neurons (n = 4 hemispheres from 3 mice). Since 84.7% of all cell bodies are shown to colocalize within the dorsal subiculum, this provides greater evidence that YFP is properly being expressed within this transgenic mouse line.

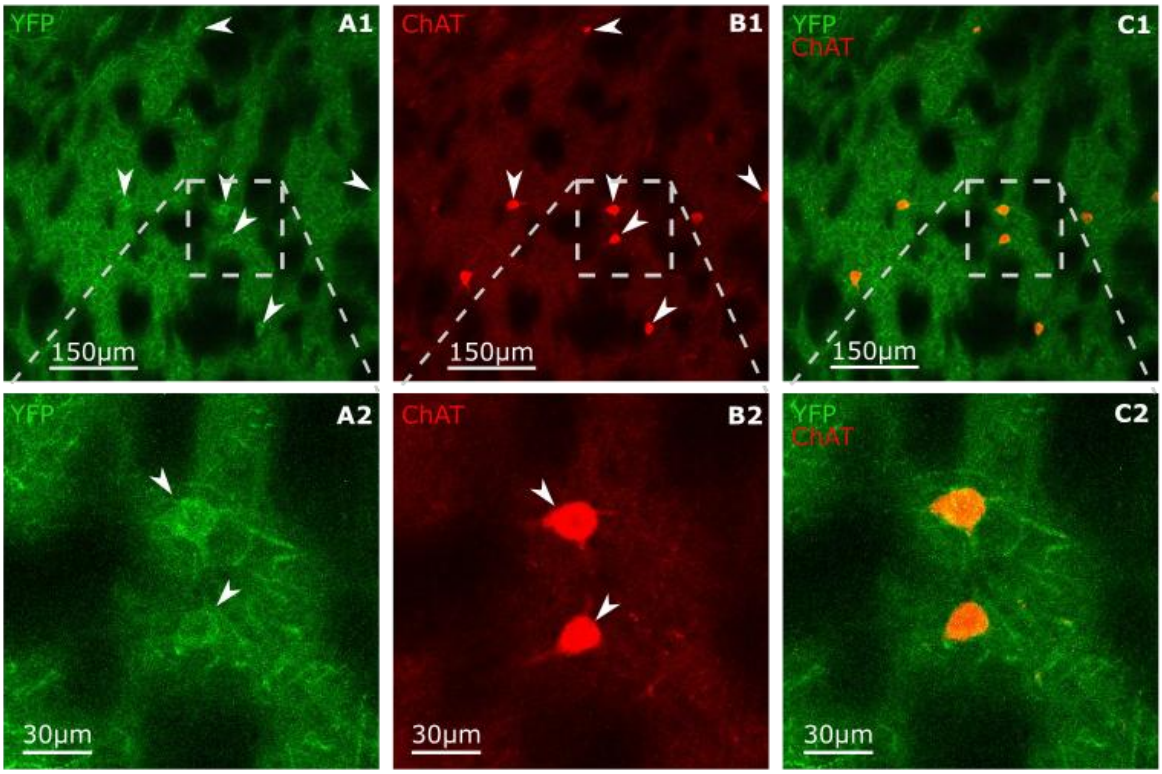

Figure 13. YFP (**A**, **C**) and ChAT (**B**, **C**) co-expression in the striatum. White arrows show cell bodies that colocalize in both YFP and ChAT images. Images were taken with a 20X objective lens with a field of view of 636.5 μm x 636.5 μm (**1**). Original images were enlarged to better display cell body colocalization (**2**). Figure created using a z-stack maximum intensity projection with a depth of 14 μm.

Table 3. Quantification of striatal neurons colocalized with ChAT, YFP, or both. YFP and ChAT images were manually compared in four hemispheres from three mice with z-stack depths varying from 23 μm to 31 μm.

	ChAT	YFP	Total colocalized
Average Number of Striatal Neurons	31.3	28.8	60
Colocalized (%)	81.2	89.3	84.7
Standard Error	1.9	1.6	0.9

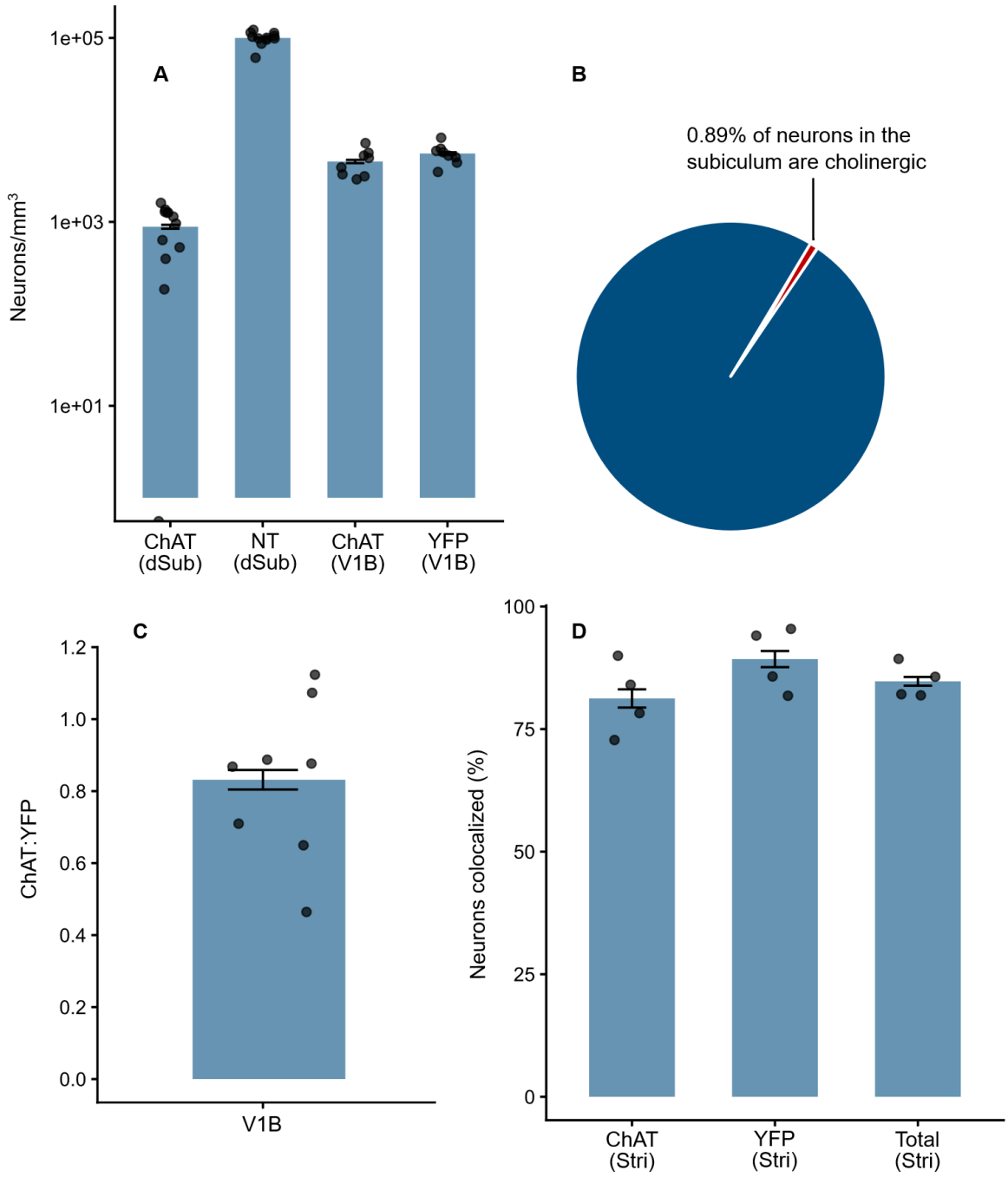

Figure 14. A) Comparing cell density from NT and ChAT-labelling in the dorsal subiculum (dSub) with YFP and ChAT-labelling in the primary visual cortex. **B**) Representation of cholinergic neurons (in red) compared to non-cholinergic neurons (in blue) in the dorsal subiculum. **C**) Ratio of ChAT-to-YFP neurons in V1B. **D**) Percentage of ChAT and YFP neurons that colocalize in the striatum, as well as the overall percentage of cell bodies that colocalize compared to the total number present.

4.0 Discussion

As the results demonstrate, YFP is properly expressed in the medial habenula, striatum, and V1B. The ChAT-to-YFP ratio in V1B is 0.83:1, and striatal neurons in both ChAT and YFP conditions colocalize 84.7% of the time. Furthermore, YFP expression allowed detailed subcellular structures to be visualized including cell bodies and neuropil structures such as dendritic spines and *en passant* synaptic boutons especially in the dorsal subiculum. All this evidence supports that ChATcre::ChR2-YFP transgenic mice properly express YFP when ChAT is synthesized in the striatum, medial habenula, and V1B. However, in the dorsal subiculum there is an abundance of YFP-expressing neuronal cell bodies while ChAT immunolabelled neurons only represent 0.89% of all neurons in the dorsal subiculum. Since there is a large discrepancy between the few ChAT cell bodies present and the overabundance of YFP expressed, we conclude that the dorsal subiculum is non-cholinergic but may have been cholinergic some time earlier in development.

4.1 ChAT labelling

Goat-anti-ChAT antibodies were found to be the best option to label cholinergic neurons in the dorsal subiculum alongside positive controls. All positive controls (the striatum, medial habenula, and V1B) showed proper colocalization between ChAT-labelled cell bodies and neurons visualized with YFP. This helps show that YFP is properly expressed from our immunolabelling of ChAT in a few brain regions demonstrated by others to express ChAT-containing neurons. Therefore, this validates the ChATcre::ChR2-YFP mouse line. Additionally, it validates the accuracy of goat-anti-ChAT in its ability to label ChAT-containing neurons. Rabbit-anti-ChAT, while not as precise in labelling neuropil, was also able to effectively label ChAT-containing neurons in the subiculum which provides further evidence that structures present are not being mislabelled.

Examining ChAT expression in the dorsal subiculum shows very few neurons labelled despite the many cell bodies visualized with YFP. The neurons that are labelled with ChAT tend to colocalize with YFP-visualized cell bodies, which offers support that this transgenic mouse line is not randomly expressing YFP. Despite this overlap, the limited number of cholinergic neurons promotes the longstanding belief that the dorsal subiculum is non-cholinergic, a notion that neuronal quantification supports.

4.2 Neuronal quantification

Cholinergic neurons were quantified and compared to the overall number of neurons in the dorsal subiculum to find the percentage of neurons that contained ChAT. The quantification of NT-labelled neurons, which represents the overall number of neurons in the dorsal subiculum, seems to be consistent with results found in the scientific literature. The mean findings within the scientific literature show the dorsal subiculum to have a density of approximately 100,318 (±39,892) neurons per mm^3 (Fabricius *et al*., 2008; Keller *et al*., 2018; Trujillo-Estrada *et al*., 2014), which aligns with the 99,941 (±1,478) neurons per mm^3 quantified in our study.

To further validate the labelling and quantification of cholinergic neurons, ChAT cell bodies in the V1B were examined. In the literature, there are few examples of cholinergic neurons in V1B having been quantified. Dudai *et al.* (2020) found that VIP-ChAT colocalization in the mouse V1B was 99.4% (±0.7%), and using VIP to estimate ChAT density, quantified 546 (±81) cholinergic neurons/mm^3. However, Kim *et al.* (2017) found a VIP density of ~3,000 neurons/mm^3 in V1B. Examining the results obtained from the previous Honour student in the Nashmi Lab shows that our ChAT density in the V1B aligns with the values previously found in male (5,447 cells/mm^3) and female mice (3,666 cells/mm^3) (unpublished). The results from Kim *et al*. (2017) also match these results, since it was found that the number of cholinergic neurons differ by sex and that female mice have fewer ChAT-labelled cell bodies. Furthermore, the ratio of ChAT-to-YFP neurons in V1B suggests that they are labelling a similar number of cell bodies, and that either YFP is slightly being overexpressed or that ChAT is unable to penetrate and label all cholinergic cells. Based on the accuracy of the labelling in other

regions, the latter option is more likely. Additionally, since most ChAT neurons colocalized with YFP cell bodies in the striatum, this increases the likelihood that YFP is not being ectopically expressed.

As cholinergic neurons in the dorsal subiculum have yet to be quantified, there are no published studies with which our results can be compared. Therefore, to our knowledge, this is the first study to quantify the density of cholinergic neurons in the dorsal subiculum. Despite this, the very sparse number of ChAT-labelled neurons compared to the overall number of neurons in the dorsal subiculum provides support that it is not a cholinergic nucleus although it appears to receive cholinergic afferents from other brain regions (Woolf, 1991).

4.3 YFP expression

Although the dorsal subiculum lacks cholinergic neurons, YFP allowed the visualization of various neuronal subcellular structures. Most notably were the dendritic spines identified along its dendrites. We were also able to visualize YFP in the axons and putative presynaptic bouton swellings that were interspersed along the fine axons and therefore resembled *en passant* presynaptic boutons. Since cholinergic cell bodies communicate with other neurons using ACh, it stands to reason that the cholinergic neurons visualized would have axons that contain ChAT especially at these sites. The dendrites visualized in our study show numerous spines emerging along their length which act as postsynaptic sites for neuronal communication. Since YFP is fused with ChR2 which is a light-activated cation channel, it allows YFP to spread throughout the neuron's extremities along the plasma membrane (Lin, 2011).

Despite this, the dorsal subiculum was still found to be non-cholinergic. This is surprising, since there is tremendous detail in the neuropil structures visualized with YFP. It is unlikely that this would be expressed through chance alone, given that all six mice expressed YFP to the same extent. Furthermore, ChAT-labelled neurons that were present would colocalize with YFP cell bodies, both in the dorsal subiculum and in our

positive cholinergic regions. Given these results, YFP is shown to be properly expressed everywhere except for the dorsal subiculum.

4.4 Possible explanations for YFP expression in ChAT-negative neurons in the dorsal subiculum

Since ChAT-labelled neurons make up less than 1% of the overall cell bodies in the dorsal subiculum, it is clear that the subiculum is largely non-cholinergic. This matches the previous literature, which has not found any evidence to suggest otherwise (Woolf, 1991). These results also align with Granger *et al*.'s findings, where a different transgenic mouse line ($ChAT^{ires\text{-}Cre}$ x $Rosa26^{lsl\text{-}tdTomato}$) strongly labeled neurons in the dorsal subiculum, yet did not express ChAT in adulthood (2020). Despite the lack of ChAT-labelled neurons, YFP is still expressed in somata, dendrites, and axons throughout the dorsal subiculum. Based on our results in the striatum, medial habenula, and V1B, YFP is largely co-expressed with ChAT immunolabelling and therefore is properly expressed in these brain regions. This seems to suggest that although the dorsal subiculum is non-cholinergic in adult mice, it may express ChAT at some point during development. Previous research has shown that it is possible for neurons to switch neurotransmitters based on the conditions present (Li *et al*., 2024). Although Li *et al*. found that fear changed neurotransmitter use from glutamate to GABA in the dorsal raphe (2024), it is possible that a similar mechanism exists during cholinergic development. This would explain why the subiculum contains ChR2 and YFP during adulthood yet does not possess any cholinergic properties. ACh has been found to enhance neurogenesis in the hippocampus and plasticity in the visual cortex, which means that ACh may act as a catalyst for subicular neuronal development (Gu & Singer, 1993; Mohapel *et al*., 2005). Therefore, it could be possible that subicular neurons expressed ChAT at one point in development but then transitioned into another neuronal type.

4.5 Future studies

Future examinations into the subiculum's cholinergic properties should be conducted during the period of development prior to adulthood. To ensure that adult mice do not express ChAT, a cre-dependent TdTomato adeno-associated virus should be injected into ChATcre::ChR2-YFP transgenic mice. Assuming cholinergic neurons begin producing other types of neurotransmitters in adulthood, TdTomato should not be found in the dorsal subiculum. Once this is confirmed, this method can also be used during multiple stages of development to see when TdTomato is expressed. Alternatively, a brute force approach to understanding when cholinergic neurons in the subiculum may change properties would be to look for YFP expression at various stages in ChATcre::ChR2-YFP development and compare when ChAT immunolabelling no longer appears.

Goral *et al*. (2019) investigated when cholinergic neurons develop and found that most are cholinergic prior to postnatal day 12. Examining the subiculum surrounding this period would be ideal, as the hippocampus and cerebral cortex begin expressing sparse cholinergic neurons (Goral *et al*., 2019). Another approach to understand the changes in cholinergic neurons would be to compare non-cholinergic neurons in the dorsal subiculum, such as those producing GABA or glutamate, with those that express YFP to see if they colocalize at any point. This would provide evidence of a neurotransmitter change at some point during development. Additional studies could also examine whether cholinergic density differs between male and female mice. While comparing the limited ChAT expression in the dorsal subiculum between adult male and female mice could be done, examining this in developing mice (where we assume ChAT-labelled neurons would properly be expressed) would help uncover any differences between male and female mice pertaining to development. Finally, using C57BL/6 mice with ChAT immunolabelling could be a good control experiment to verify the expression of cholinergic neurons compared to ChATcre::ChR2-YFP mice.

4.6 Study limitations

While this study sought to investigate the cholinergic properties of the dorsal subiculum, there are some limitations. The way in which neuronal density was calculated may not perfectly reflect the true number of neurons found *in vivo*. The method for quantifying neurons was a calculated estimate based on thresholding the NT signal, totalling this signal in the volume imaged in the field of view, and obtaining the mean areas of a number of NT-labelled neurons in an optical slice to estimate the mean volume per neuron, assuming a spherical shape of each neuron. Moreover, the watershed algorithm may not fully separate neurons from other cell bodies or neuropil, and certain thresholds could improperly label neurons. Since quantification of non-NT-labelled neurons was done manually, errors could have occurred through human counts. The densities quantified may also be skewed as fixation is known to shrink brain volumes (Bolduan *et al*., 2020). Finally, this study's limited examination of the dorsal subiculum prevented us from analysing the complete rostral-caudal extent of the subiculum and whether it also expressed cholinergic neurons during adulthood. Future investigations should keep these limitations in mind.

5.0 Conclusions

This study has confirmed that neurons in the dorsal subiculum are almost entirely non-cholinergic within adult mice. Despite YFP's unusual appearance in the subiculum, it is properly expressed in the striatum, medial habenula, and V1B, providing evidence that ChATcre::ChR2-YFP mice are not ectopically inducing YFP expression. Furthermore, the detail of neuropil visualized with YFP also supports this. The evidence from this study points towards the possibility that cholinergic neurons were present in juvenile mice but were no longer expressed in adults. Exploring the subiculum's cholinergic properties during development may explain YFP's appearance despite the lack of ChAT, as well as some of its functional roles in developing mice.

References

Allen Brain Atlas. n.d. Mouse brain - Reference atlas [Online]. Available: https://mouse.brain-map.org/static/atlas [2026, March 29].

Aggleton, J. P. and K. Christiansen. **2015**. The subiculum. Pp. 65–82 in: *Progress in Brain Research*, **219,** S. O'Mara and M. Tsanov, eds. Elsevier. https://doi.org/10.1016/bs.pbr.2015.03.003.

Aosaki, T., M. Miura, T. Suzuki, K. Nishimura, and M. Masuda. 2010. Acetylcholine–dopamine balance hypothesis in the striatum: An update. *Geriatrics & Gerontology International* **10:** S148–57. https://doi.org/10.1111/j.1447-0594.2010.00588.x.

Barnett, S. C., L. C. Parr-Brownlie, B. A. L. Perry, C. K. Young, H. E. Wicky, S. M. Hughes, N. McNaughton, and J. C. Dalrymple-Alford. **2021**. Anterior thalamic nuclei neurons sustain memory. *Current Research in Neurobiology* **2:** 100022. https://doi.org/10.1016/j.crneur.2021.100022.

Bartlett, W. and G. Banker. 1984. An electron microscopic study of the development of axons and dendrites by hippocampal neurons in culture. I. Cells which develop without intercellular contacts. *Journal of Neuroscience* **4:** 1944–1953. https://doi.org/10.1523/JNEUROSCI.04-08-01944.1984.

Bolduan, F., S. Grosser, and I. Vida. 2020. Minimizing shrinkage of acute brain slices using metal spacers during histological embedding. *Brain Structure and Function* **225:** 2577-2589. https://doi.org/10.1007/s00429-020-02141-3.

Broks, P., G. C. Preston, M. Traub, P. Poppleton, C. Ward, and S. M. Stahl. 1988. Modelling dementia: Effects of scopolamine on memory and attention. *Neuropsychologia* **26:** 685–700. https://doi-org.ezproxy.library.uvic.ca/10.1016/0028-3932(88)90004-8.

Calabresi, P., B. Picconi, L. Parnetti, and M. D. Filippo. 2006. A convergent model for cognitive dysfunctions in Parkinson's disease: the critical dopamine–acetylcholine synaptic balance. *The Lancet Neurology* **5:** 974–983. https://doi.org/10.1016/S1474-4422(06)70600-7.

Coimbra, B., A. V. Domingues, C. Soares-Cunha, R. Correia, L. Pinto, N. Sousa, and A. J. Rodrigues. 2021. Laterodorsal tegmentum–ventral tegmental area projections encode positive reinforcement signals. *Journal of Neuroscience Research* **99:** 3084–3100. https://doi.org/10.1002/jnr.24931.

Commins, S., J. P. Aggleton, and S. M. O'Mara. 2002. Physiological evidence for a possible projection from dorsal subiculum to hippocampal area CA1. *Experimental Brain Research* **146:** 155–160. https://doi.org/10.1007/s00221-002-1158-x.

Dani J. A. 2015. Neuronal nicotinic acetylcholine receptor structure and function and response to nicotine. Pp. 3–19 in: *International Review of Neurobiology*, **124,** M. De Biaisi, eds. Academic Press. https://doi.org/10.1016/bs.irn.2015.07.001.

Dudai, A., N. Yayon, V. Lerner, G. Tasaka, Y. Deitcher, K. Gorfine, N. Niederhoffer, A. Mizrahi, H. Soreq, and M. London. 2020. Barrel cortex VIP/ChAT interneurons suppress sensory responses in vivo. *Public Library of Science Biology* **18.** https://doi.org/10.1371/journal.pbio.3000613.

Eickhoff, S., L. Franzen, A. Korda, H. Rogg, V.-N. Trulley, S. Borgwardt, and M. Avram. 2022. The basal forebrain cholinergic nuclei and their relevance to schizophrenia and other psychotic disorders. *Frontiers in Psychiatry* **13:** 909961. https://doi.org/10.3389/fpsyt.2022.909961.

Fabricius, K., G. Wörtwein, and B. Pakkenberg. 2008. The impact of maternal separation on adult mouse behaviour and on the total neuron number in the mouse hippocampus. *Brain Structure and Function* **212:** 403–416. https://link.springer.com/article/10.1007/s00429-007-0169-6.

Franklin, B. J. and G. Paxinos. 2008. *The Mouse Brain in Stereotaxic Coordinates*, Compact 3rd edition. Elsevier.

Granger, A. J., W. Wang, K. Robertson, M. El-Rifai, A. F. Zanello, K. Bistrong, A. Saunders, B. W. Chow, V. Nuñez, M. T. García, C. C. Harwell, C. Gu, and B. L. Sabatini. 2020. Cortical ChAT+ neurons co-transmit acetylcholine and GABA in a target- and brain-region-specific manner. *eLife* **9.** https://elifesciences.org/articles/57749.

Gu, Q. and W. Singer. 1993. Effects of intracortical infusion of anticholinergic drugs on neuronal plasticity in kitten striate cortex. *European Journal of Neuroscience* **5:** 475–85. https://doi.org/10.1111/j.1460-9568.1993.tb00514.x.

Haun, F., T. C. Eckenrode, and M. Murray. 1992. Habenula and thalamus cell transplants restore normal sleep behaviours disrupted by denervation of the interpeduncular nucleus. *The Journal of Neuroscience* **12:** 3282–3290. https://doi.org/10.1523/JNEUROSCI.12-08-03282.1992.

Huang, Q., C. Liao, F. Ge, J. Ao, and T. Liu. 2022. Acetylcholine bidirectionally regulates learning and memory. *Journal of Neurorestoratology* **10:** 100002. https://doi.org/10.1016/j.jnrt.2022.100002.

Inkscape Project. 2026. Inkscape [Software]. Retrieved from https://inkscape.org.

Keller, D., C. Erö, and H. Markram. 2018. Cell densities in the mouse brain: A systematic review. *Frontiers in Neuroanatomy* **12**. https://doi.org/10.3389/fnana.2018.00083.

Kim, Y, G. R. Yang, K. Pradhan, K. U. Venkataraju, M. Bota, L. C. García del Molino, G. Fitzgerald, K. Ram, M. He, J. M. Levine, P. Mitra, Z. J. Huang, X. J. Wang, and P. Osten. 2017. Brain-wide maps reveal stereotyped cell-type-based cortical architecture and subcortical sexual dimorphism. *Cell* **171:** 456–469. https://doi.org/10.1016/j.cell.2017.09.020.

Klinkenberg, I. and A. Blokland. 2011. A comparison of scopolamine and biperiden as a rodent model for cholinergic cognitive impairment. *Psychopharmacology* **215:** 549–566. https://doi.org/10.1007/s00213-011-2171-1.

Li, H. Q., W. Jiang, L. Ling, M. Pratelli, C. Chen, V. Gupta, S. K. Godavarthi, and N. C. Spitzer. 2024. Generalized fear after acute stress is caused by change in neuronal cotransmitter identity. *Science* **383:** 1252–1259. https://doi.org/10.1126/science.adj5996.

Lin, J. Y. 2011. A user's guide to channelrhodopsin variants: Features, limitations and future developments. *Experimental Physiology* **96:** 19–25. https://doi.org/10.1113/expphysiol.2009.051961.

Mohapel, P., G. Leanza, M. Kokaia, and O. Lindvall. 2005. Forebrain acetylcholine regulates adult hippocampal neurogenesis and learning. *Neurobiology of Aging* **26:** 939–946. https://doi.org/10.1016/j.neurobiolaging.2004.07.015.

Molecular Probe. 2003. NeuroTrace™ fluorescent Nissl stains [Online]. Available: https://documents.thermofisher.com/TFS-Assets/LSG/manuals/mp21480.pdf [March 29, 2026].

Muzio, M. R., A. O. Fakoya, and M. Cascella. 2022. *Histology, Axon.* StatPearls Publishing, Treasure Island. Available: https://www.ncbi.nlm.nih.gov/books/NBK554388/ [2022, November 14].

Posit team. 2026. RStudio: Integrated development environment for R. *Posit Software, PBC*, Boston. http://www.posit.co/.

Ruan, Y., K.-Y. Li, R. Zheng, Y.-Q. Yan, Z.-X. Wang, Y. Chen, Y. Liu, J. Tian, L.-Y. Zhu, H.-F. Lou, *et al.* 2022. Cholinergic neurons in the pedunculopontine nucleus guide reversal learning by signaling the changing reward contingency. *Cell Reports* **38.** https://doi.org/10.1016/j.celrep.2022.110437.

Runge, K., C. Cardoso, and A. de Chevigny. 2020. Dendritic spine plasticity: Function and mechanisms. *Frontiers in Synaptic Neuroscience* **12.** https://doi.org/10.3389/fnsyn.2020.00036.

Salas, R., R. Sturm, J. Boulter, and M. De Biasi. 2009. Nicotinic receptors in the habenulo-interpeduncular system are necessary for nicotine withdrawal in mice. *Journal of Neuroscience* **29:** 3014–3018. https://doi.org/10.1523/JNEUROSCI.4934-08.2009.

Sam, C. and B. Bordoni. 2023. *Physiology, Acetylcholine*. StatPearls Publishing, Treasure Island. Available: https://www.ncbi.nlm.nih.gov/books/NBK557825/ [2025, September 20].

Sandyk, R. 1991. Relevance of the habenular complex to neuropsychiatry: A review and hypothesis. *International Journal of Neuroscience* **61:** 189–219. https://doi.org/10.3109/00207459108990738.

Schneider, C. A., W. S. Rasband, and K. W. Eliceiri. 2012. 25 years of image analysis. *Nature Methods* **9:** 671–675. https://doi.org/10.1038/nmeth.2089.

Trujillo-Estrada, L., J. C. Dávila, E. Sánchez-Mejias, R. Sánchez-Varo, A. Gomez-Arboledas, M. Vizuete, J. Vitorica, and A. Gutiérrez. 2014. Early neuronal loss and axonal/presynaptic damage is associated with accelerated amyloid-β accumulation in AβPP/PS1 Alzheimer's disease mice subiculum. *Journal of Alzheimer's Disease* **42:** 521–41. https://doi.org/10.3233/JAD-140495.

Villano I, A. Messina, A. Valenzano, F. Moscatelli, T. Esposito, V. Monda, M. Esposito, F. Precenzano, M. Carotenuto, A. Viggiano, S. Chieffi, G. Cibelli, M. Monda, and G. Messina. 2017. Basal forebrain cholinergic system and orexin neurons: Effects on attention. *Frontiers in Behavioural Neuroscience* **11**. https://doi.org/10.3389/fnbeh.2017.00010.

Woolf, N. 1991. Cholinergic systems in mammalian brain and spinal cord. *Progress in Neurobiology* **37:** 475–524. https://doi.org/10.1016/0301-0082(91)90006-M.

Appendix A: Cre-labelling

To examine if cre-recombinase, and thus ChAT, is expressed in the adult dorsal subiculum, we first compared cre labelling with YFP expression and ChAT-labelling in the striatum (Figure A1). Cre was visualized using rabbit-anti-cre (Biolegend, cat # 908001) & donkey-CY5-anti-rabbit, and was compared to goat-anti-ChAT (Millipore, cat # AB144P) and donkey-Cy3-anti-goat. Cre was excited using 438 nm wavelengths, and required spectral unmixing to separate CY3, YFP, and autofluorescence. While YFP and ChAT both visualized cell bodies, cre did not label any neurons. The lack of cre-expression in a known cholinergic region implies that this antibody was unable to properly label cre. Due to limited time and the lack of results that this antibody produced, only one hemisphere was analyzed for cre-expression.

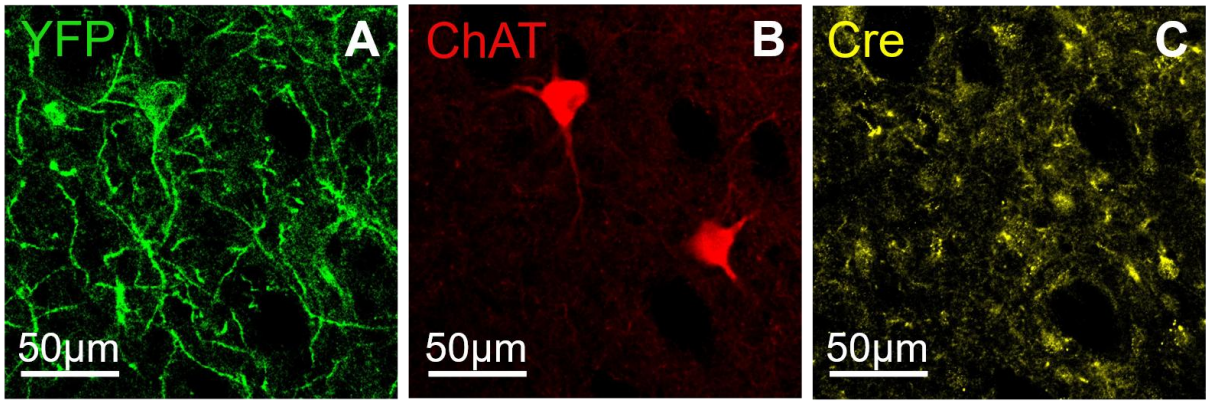

Figure A1. Images of striatal cholinergic neurons using YFP (**A**), ChAT (**B**), and cre (**C**) labelling with a 20X objective lens and a field of view of 199.86 µm x 199.86 µm.

Appendix B: ChAT/NT Colocalization

To further validate the proper labelling of cholinergic neurons, we tried imaging subicular slices with both NT and ChAT-labelled neurons. The basis for this experiment was that if ChAT neurons colocalized with NT-labelled cell bodies in the subiculum, this would strengthen the evidence that the few cholinergic neurons present are being properly labelled. Adding NT onto the subicular slice alongside either the primary or secondary antibodies for ChAT led to very poor images (Figure B1). After checking the Molecular Probes (2003) online manual for NT, it appears that various blocking solutions can quench the fluorescence of Nissl stains. While donkey serum was not mentioned in the list of blocking solutions, it is entirely possible that it affected NT labelling. To combat this, we added NT after having added primary and secondary antibodies with a PBS wash to remove the donkey serum. While NT-labelling had improved, ChAT-labelling was very limited, perhaps having been washed off with the extra PBS rinse (data not shown). This experiment was limited in both time and samples examined. Additional troubleshooting should be done to ensure ChAT and NT colocalize completely.

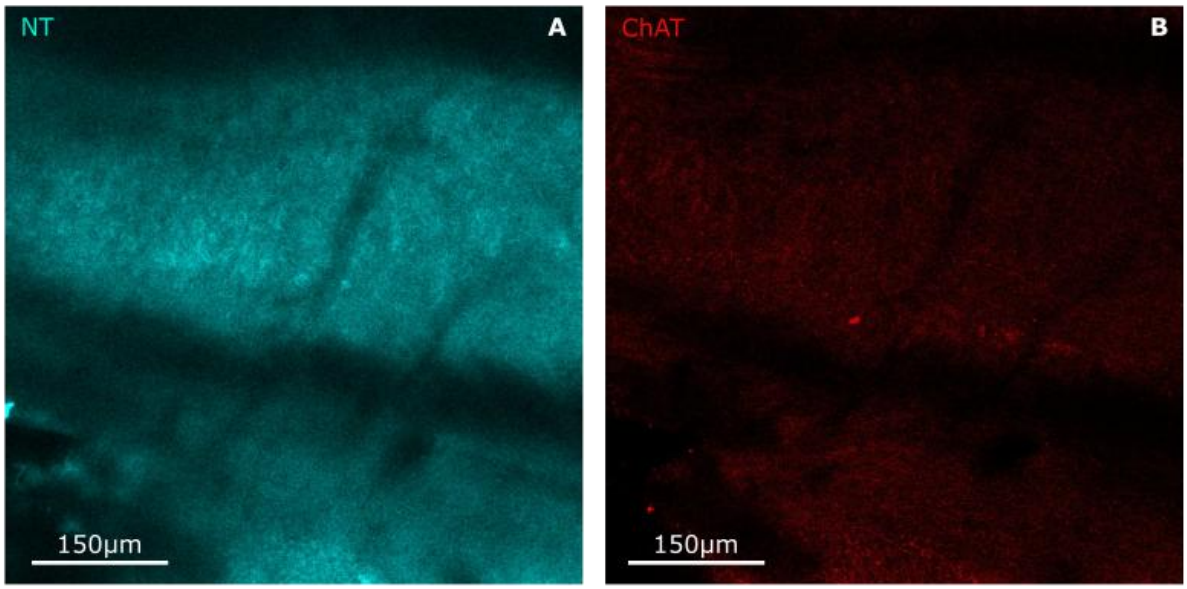

Figure B1. NT (**A**) and ChAT (**B**) co-labelling in the dorsal subiculum with a 20X objective lens and a field of view of 636.6 µm x 636.5 µm. Figure created using a z-projection with a depth of 13 µm.